

REVIEW

Photoinduced generation of the second harmonic in centrosymmetric media

To cite this article: Evgenii M Dianov and D S Starodubov 1995 *Quantum Electron.* **25** 395

View the [article online](#) for updates and enhancements.

You may also like

- [\(Invited\) Use of Discrete Liquid-Solid Contact Electrification As Ways of Self-Powered Sensing](#)
Dong Sung Kim
- [Rheological Model of the Full Flow Curve of Highly Viscous and Solidifying Oil at Starting and Steady-State Mode Conditions](#)
R M Karimov, R R Tashbulatov and R U Rabaev
- [Micelle Mediated Extraction of Neodymium and Electrochemical Characterization of AOT Reverse Micelles](#)
Shannon Anderson, Egwu Eric Kalu, Clayton Clark et al.

Photoinduced generation of the second harmonic in centrosymmetric media

E M Dianov, D S Starodubov

Abstract. This review deals with the photoinduced generation of the second harmonic in centrosymmetric media. A brief account is given of the main results of the reported investigations. The models proposed to describe the effect are discussed. The principles for experimental separation of the contributions of the various mechanisms are put forward and the results of the relevant experiments are described. A detailed phenomenological description of the photogalvanic mechanism is given and an experimental confirmation of this mechanism is reported.

1. Introduction

Generation of the second harmonic of optical radiation is one of the most thoroughly studied nonlinear effects, which has stimulated the subsequent extensive growth of nonlinear optics. The discovery by Franken et al. [1] of the frequency doubling of ruby laser radiation in a quartz crystal has been followed by an enormous number of investigations of the effect and by the development of efficient frequency doublers of laser radiation operating in a wide spectral range from UV to IR.

Optical harmonic generation is described by equations that relate the polarisation P of a medium to the electric field E . If the optical radiation intensity is sufficiently high, so that the optical field E approaches the internal atomic field $E_{at} \sim 10^8 - 10^9 \text{ V cm}^{-1}$, the relationship between the polarisation P and the field E becomes nonlinear. If $E/E_{at} \ll 1$, the polarisation response considered in the electric-dipole approximation can be represented as a series expansion in powers of the perturbing field:

$$P = P_{lin} + P_{nl} = \epsilon_0 (\chi^{(1)} E + \chi^{(2)} EE + \chi^{(3)} EEE + \dots), \quad (1)$$

$\chi^{(n)}$ is the n th-order susceptibility of the medium, which is a tensor of rank $n + 1$; ϵ_0 is the permittivity of vacuum. The first term of expansion (1) describes the linear polarisation response of the medium, where $\chi^{(1)}$ is related to the permittivity of the medium ϵ and its refractive index n by $n^2 = \epsilon = 1 + \chi^{(1)}$.

The second term is the first component of the nonlinear response characterised by the quadratic nonlinear

susceptibility $\chi^{(2)}$ responsible for second-order nonlinear processes, including second harmonic generation (SHG).

The intensity of the second harmonic, generated in an optically transparent medium of thickness L , is

$$I_{2\omega} \propto (\chi^{(2)})^2 L^2 \left[\frac{\sin(L\Delta k/2)}{\Delta k/2} \right]^2 I_{\omega}^2, \quad (2)$$

where $\Delta k = k_{2\omega} - 2k_{\omega} = 2\pi/\Lambda$ is the phase mismatch between the fundamental-frequency (pump) and second-harmonic waves; $\Lambda = \lambda/2(n_{2\omega} - n_{\omega})$ is the period of spatial oscillations of the second-harmonic radiation (doubled coherence length); n_{ω} and $n_{2\omega}$ are the refractive indices of the medium for the pump and second-harmonic waves, respectively; λ is the pump wavelength. Efficient frequency doubling requires that two conditions be satisfied: $\chi^{(2)} \neq 0$ (existence of the quadratic susceptibility) and $\Delta k = 0$ (phase-matching condition).

The quadratic susceptibility does not exist in centrosymmetric media in the electric-dipole approximation. The symmetry of such a medium can be broken in a strong electric field. Then the quadratic susceptibility, proportional to the electric field, and the cubic susceptibility appear in a material with a cubic nonlinearity. Terhune et al. [2] were the first to observe SHG in a centrosymmetric medium (a calcite crystal) subjected to a static electric field.

Glass is a centrosymmetric medium, so that in the electric-dipole approximation it does not have the quadratic susceptibility essential for efficient SHG. In addition to the second-order electric dipole contribution to the nonlinear polarisation, there are also higher-order—especially the most important quadrupole, magnetic-dipole, and surface—contributions, but SHG is then very weak [3]. There have been reports also of SHG and of sum-frequency generation, the low efficiency of which has been attributed to higher-order nonlinearities [4, 5].

In 1986 Österberg and Margulis [6] reported efficient photoinduced SHG in a fibre waveguide made of germanium-doped silica glass after this fibre had been subjected to prolonged irradiation by a YAG:Nd laser. This result stimulated considerable interest: many laboratories and scientific centres throughout the world are now studying intensively this effect. The interest in the photoinduced SHG is enhanced by the possibility of constructing practical frequency doublers from inexpensive and widely accessible glass fibre waveguides. Low-cost compact sources of blue–green radiation for data storage systems, based on laser diodes and glass fibre waveguides, are attracting particular attention. Moreover, bulk glasses with the photoinduced SHG look promising as erasable data storage media [7].

E M Dianov, D S Starodubov Fibre Optics Scientific Centre at the Institute of General Physics, Russian Academy of Sciences, Moscow

Received 8 September 1994

Kvantovaya Elektronika 22 (5) 419–432 (1995)

Translated by A Tybulewicz

Since this first report in 1986, over 200 papers have been published but a full physical picture of the effect is still lacking. Several review papers have been devoted to SHG in glasses, but they cover work done only up to 1990 [8–11]. However, the last few years have brought new results which throw light on the mechanisms of the induced quadratic susceptibility of glasses. Moreover, some new glasses have been prepared in which efficient SHG is possible. It is therefore opportune to rethink and review the results obtained in the last few years.

The present review is organised as follows. Section 2 gives a brief historical review of the work done on the photo-induced SHG: it covers the most important (in our opinion) research results and deals with the models proposed to account for them. Section 3 deals with the investigations that throw light on the physical mechanisms responsible for the quadratic susceptibility, and Section 4 describes new glass compositions which are promising for SHG. Section 3 consists largely of our own results.

2. Brief historical review

As pointed out in the Introduction, Österberg and Margulis were the first to report in 1986 [6] efficient SHG of laser radiation with the wavelength $\lambda = 1.06\ \mu\text{m}$ in glass fibre waveguides. Excitation of a single-mode fibre waveguide with radiation from a Q-switched and mode-locked YAG:Nd laser revealed an increase in the second harmonic signal during a period of about 12 h. This increase, under the action of radiation at the fundamental frequency of a laser (pump radiation), is called self-preparation (self-organisation) of a fibre waveguide.

In these experiments use was made of a commercial germanium-doped waveguide and the peak pump power in this waveguide was 20 kW. When saturation was reached, SHG efficiency was 3%–5%, which was sufficient to pump a dye laser [6, 12]. Such a high conversion efficiency in a 50 cm-long fibre implied breaking of the symmetry of glass and simultaneous satisfaction of the phase-matching condition.

Farries et al. [13] observed efficient ($\sim 1\%$) SHG from YAG:Nd laser radiation in a fibre waveguide doped with Ge (15%) and phosphorus (less than 1%). When this waveguide was pumped by pulses of duration less than 100 ps and of 10 kW peak power, the peak second-harmonic power increased from 100 pW to 50 W in 10 h.

Farries et al. [13] postulated a physical mechanism of efficient SHG involving formation of a spatial grating of dipole colour centres with a period satisfying the phase-matching condition. The colour centres, which enhanced the quadratic nonlinearity, were formed by the second-harmonic radiation generated because of the quadrupole contribution to the nonlinear polarisation. The formation of a spatial grating of $\chi^{(2)}$ in a fibre waveguide was supported by measurements of the spectral width of the phase-matching curve, which was 0.24 nm. Subsequently, formation of a grating of the quadratic susceptibility in a fibre waveguide had been confirmed in a whole series of experiments [14–18] and is now generally accepted.

Terhune and Weinberger [3] estimated the efficiency of SHG in glass fibre waveguides due to the contribution of the core–cladding interface and due to the quadrupole nonlinearity. Estimates indicate that, even when the phase-matching condition is satisfied, the maximum conversion

efficiency does not exceed 10^{-5} and cannot account for the experimental results.

A major step in the solution of the problem of the photo-induced SHG was made by the model of Stolen and Tom [19], in which an alternating-sign grating of $\chi^{(2)}$ appears because of orientation of defects by the zero-frequency polarisation. This polarisation is created by mixing of the pump and second-harmonic waves due to the cubic nonlinearity. This mechanism is analogous to optical rectification. The zero-frequency polarisation oscillates along the length of a fibre waveguide with a period corresponding to the condition of phase matching of the pump and second-harmonic waves. In other words, self-organisation of the quadratic nonlinearity takes place and this automatically deals with the mismatch of the phase velocities of the pump and second-harmonic waves in a fibre waveguide.

Stolen and Tom used this model [19] to propose and carry out an SHG experiment in which seeding second-harmonic radiation was coupled into a waveguide together with the fundamental-frequency (pump) radiation. As a result, efficient SHG and, consequently, a grating of $\chi^{(2)}$ appeared in the fibre waveguide after just 5 min (in previous experiments where such second-harmonic seeding radiation was not used, SHG appeared after many hours). We shall show later that the model of Stolen and Tom does not, in general, account for the photoinduced SHG in fibre waveguides, but it leads to a fruitful idea of the feasibility of using seeding second-harmonic radiation to prepare ('write') a grating of $\chi^{(2)}$. A successful experimental realisation of this idea was the reason why the work of Stolen and Tom had a major influence on the subsequent development of models designed to account for the nature of the photoinduced quadratic nonlinearity, and led to the development of orientational models [20–26].

Ouellette et al. [27] have demonstrated that a quadratic nonlinearity grating formed in a fibre waveguide by the fundamental-frequency radiation from a YAG:Nd laser and its second harmonic can be erased optically. This was done by the second harmonic of the YAG:Nd laser or by radiation from an argon laser. The nonexponential time dependence of the erasure process is explained in Ref. [27] by a model postulating separation of charges during grating formation and charge recombination during erasure. According to this model, such charge separation occurs in a constant electric field generated by mixing of the fundamental-frequency and second-harmonic waves due to the cubic nonlinearity. Charge accumulation at the boundary of the illuminated region creates an electrostatic field which gives rise to a nonzero quadratic nonlinearity. Although this model, like that proposed by Stolen and Tom [19], accounts for the appearance of a nonlinearity by postulating optical mixing, the idea of macroscopic separation of charges and the experimental results [27] supporting this idea have proved an important step in the path towards understanding of the mechanism of the photoinduced SHG in fibre waveguides.

An intense contradiction in the models postulating mixing of the pump and second-harmonic waves due to a cubic nonlinearity was pointed out by Mizrahi et al. [28, 29]. Their estimate of the optical rectification field gave peak intensities of the order of $1\ \text{V cm}^{-1}$, clearly insufficient for the orientation of dipoles. A comparison of the experimental induced quadratic nonlinearities obtained at very different intensities (Q switching with and without

mode locking) led Mizrahi et al. [28, 29] to the conclusion that the induced nonlinearity is near the saturation point. This observation and an estimate of the optical rectification field led them to propose and check experimentally an optical rectification model [28, 29].

The intention of their experiment was to saturate the nonlinearity by a stronger homogeneous field and to suppress a weak spatially oscillating contribution. Then, instead of a grating of $\chi^{(2)}$, ensuring phase-matched SHG, a homogeneous quadratic nonlinearity region should form along the fibre waveguide and the SHG efficiency should decrease significantly because of the loss of phase matching. This experiment showed that a field of 2.5 kV cm^{-1} intensity had practically no effect on the SHG efficiency [29] and it demonstrated the unsatisfactory nature of the models based on mixing of the pump and second harmonic by a cubic nonlinearity.

In 1989, Dianov et al. proposed [17] a fundamentally new charge model of the effect. They postulated that an electrostatic field which appears in a medium is not weak, but strong (10^4 – 10^5 V cm^{-1}). This field is the result of the coherent photogalvanic effect caused by quantum interference between the following photoionisation processes: one-photon ionisation by the second harmonic and two-photon ionisation by the pump radiation. This process is asymmetric and it creates a coherent photocurrent. Separation of charges and their capture by traps at the boundary of the illuminated region creates a strong electrostatic field which oscillates along a fibre waveguide with a periodicity necessary for the phase-matched SHG. In its turn, this field creates a quadratic susceptibility grating [30, 31]. The coherent photogalvanic effect due to free carriers was first considered theoretically by Baskin and Éntin [32] and then by Éntin alone [33] for the case of photoionisation.

Baranova et al. [34] made a considerable contribution to the understanding of the physical reason for the appearance of a photoionisation asymmetry in the field of an optical wave. They demonstrated that the fundamental-frequency and second-harmonic fields have a nonzero value of the average cube $\langle E_\omega E_\omega E_{2\omega}^* \rangle$. The emission of photoelectrons is most probable at the field maxima, which are considerably greater along one of the directions. Therefore, a field of this type creates a strongly asymmetric photoionisation. The dependence of the direction of electron emission on the phases of the waves with the frequencies ω and 2ω creates a spatially oscillating coherent photocurrent [17, 33, 34]. These conclusions were supported by an experimental demonstration of an asymmetry of electron emission from a photomultiplier photocathode [34] and by asymmetric photoionisation in sodium vapour [35].

Anderson et al. [36] also proposed a model based on the appearance of a photogalvanic current under the influence of waves of frequencies ω and 2ω . However, in contrast to the model of the lowest-order coherent photogalvanic effect [17, 34], Anderson et al. [36] considered higher orders of the coherent photocurrent due to the interference of two-photon, three-photon, and four-photon ionisation processes. According to them [36], the proposed mechanism provides a better description, for energy reasons, of the photoionisation of germanium defects with a band in the region of 5 eV.

The appearance of a number of photogalvanic models describing the main experimental relationships has not solved the problem of whether models of the orientational

type or those based on charge separation (charge models) are correct. A serious argument in support of the charge models was provided by Mizrahi et al. [37]. They investigated the tensor properties of the induced quadratic nonlinearity and obtained a relationship between the tensor components which agrees very well with the models postulating macroscopic charge separation: $\chi_{xxx}^{(2)} = 3\chi_{xyy}^{(2)}$. However, it has since been shown that the tensor measurements do not provide unambiguous evidence in support of the charge models. An analysis of the microscopic symmetry of defects in glass can also account for the results obtained on the basis of the orientational models [25].

Margulis et al. [38] proposed an original water cell method for measuring the phase shift between the seeding second-harmonic radiation and the photoinduced second harmonic. Their measurements showed that when a grating involving strong seeding radiation is formed in a waveguide, the phase of the photoinduced second harmonic differs by $\sim \pi/2$ from the seeding radiation phase, demonstrating that the response of the medium is local. Here the term 'local' means that the extrema of a quadratic nonlinearity grating coincide with the extrema of the interference pattern of the optical field. (The use of a dichroic mirror led to an error of π in the phase of the first determination, so that Margulis et al. [38] were unable to determine the sign of the phase difference.) Similar (apart from the sign) results have been obtained for fibre waveguides by Koch and Moore [39], and also by Bolshtyansky et al. [40] for bulk glasses.

Dianov et al. [31, 41] proposed and confirmed experimentally a dynamic model of amplification of weak seeding second-harmonic radiation in fibre waveguides. They used the experimental results [38, 39], demonstrating the local nature of the response of the medium, to suggest and verify experimentally [31, 41] the existence of a dynamic phase mismatch between a grating and an interference pattern of optical fields when the grating is formed in the presence of weak seeding radiation. This mismatch appears because of the inertia (slow response) of the grating erasure process and it ensures amplification of the initial SHG. At saturation this mismatch reaches $3\pi/4$ because of the dynamic amplification mechanism. A temperature-induced phase shift of the grating to $\pi/2$ makes it possible to double the SHG efficiency at saturation [41]. Krol et al. demonstrated [42] that the stability of the phase relationships between the waves with the frequencies ω and 2ω is important in the formation of a grating in fibre waveguides: the occurrence of phase fluctuations during the propagation of waves with frequencies ω and 2ω along different paths reduces the efficiency of the process by three orders of magnitude [42]. Lawandy and Selker [43] observed the photoinduced SHG in bulk fibre preforms and Zel'dovich et al. [44] found this effect in bulk glasses: these are important results which should help to settle the problem of the macroscopic nature of the photoinduced nonlinearity.

Experimental investigations of the spatial distribution of the intensity of the photoinduced second harmonic, which have made it possible to visualise space charge regions [45], have led to the development of a clear method involving displacement of a sample in the course of formation of a grating. This method can be used to decide which of the macroscopic models (orientational or charge) describes the appearance of a $\chi^{(2)}$ grating [46]. Motion of space charge regions in the course of formation of quadratic susceptibility

gratings has been demonstrated, studies have been made of the dynamics of second harmonic spots in the near- and far-field zones on the basis of phase relationships, and spatial distribution of the charge density has been modelled [47].

The distribution of an electrostatic field, determined later by Dominic and Feinberg [48] from the distribution of a quadratic nonlinearity by a more detailed scanning of a region subjected once to the process (without displacement of a sample in the course of grating formation by the fundamental-frequency and second-harmonic radiations), has provided further clear confirmation of the observed macroscopic charge separation [46]. Carvalho et al. [49] studied the influence of UV radiation (fourth harmonic of a YAG:Nd laser) on the formation of quadratic nonlinearity gratings in germanium-doped fibre waveguides. They found that ultraviolet irradiation increases the rate of growth and the saturation level of the second-harmonic signal. They used their experimental results [49] to draw the important conclusion that UV radiation can not only generate defects, but also fill metastable states.

Ouellette et al. [50] discovered that exposure of fibre waveguides to a hydrogen atmosphere increased the efficiency of the photoinduced SHG. Krol et al. [51] carried out a luminescence analysis of fibre waveguides exposed to hydrogen and attributed the observed increase in the photoinduced SHG efficiency to an increase in the concentration of Ge-H centres. According to Krol et al. [51], this type of defect should give rise to the lowest-order coherent photogalvanic effect because of photoionisation involving one second-harmonic photon and two fundamental-frequency photons. Subsequently Krol et al. observed [52, 53] a resonant increase in the photoinduced SHG efficiency by thulium doping of fibre waveguides, demonstrating the participation of intermediate states in the photoionisation process.

The linearity of the initial rise of the photoinduced quadratic nonlinearity in fibre waveguides was demonstrated experimentally by Kamal et al. [54]. They proposed to determine the order of the process from the dependence of the initial growth rate on the intensity of the grating-forming waves. The results obtained agreed with the multiphoton model of a coherent photocurrent created by interference between two-photon absorption of the second harmonic and three-photon absorption involving one second-harmonic photon and two fundamental-frequency photons. The results of similar investigations carried out by Dominic and Feinberg [55] on a fibre preform also agreed better with the multiphoton model [36] than with the model of the lowest-order coherent photocurrent [17]. Dominic and Feinberg ignored [55] the influence of filling of intermediate states on the order of the process.

Lawandy and MacDonald [56–59] discovered and investigated the photoinduced SHG in glasses containing semiconductor nanocrystallites (also called microcrystallites) [56–59]. Physical and nonlinear-optical characteristics of such glasses differed considerably from those consisting of a single phase [46, 56]. Estimates of the optical rectification field inside these semiconductor nanocrystallites were used by Lawandy and MacDonald in a discussion of the problem of charge transfer in an optical rectification field, accompanied by the capture in traps near the glass–semiconductor interfaces [56, 58]. An alternative approach was proposed by Dianov et al. [46], who considered the coherent photogalvanic effect in nanocrystallites.

Investigations of the influence of temperature on the photoinduced SHG have demonstrated the possibility of existence of the coherent photogalvanic effect because of the presence of thermalised carriers in nanocrystallites [60]. Experiments involving ‘reading’ of the photoinduced nonlinearity at the moment of action of a ‘write’ pulse support the photogalvanic origin of the photoinduced quadratic nonlinearity in glasses containing semiconductor nanocrystallites [61, 62].

Efficient photoinduced SHG has been observed in cerium-doped lead germanate glasses [63]. These glasses can be prepared at fairly low densities of the write power and are promising media for practical devices.

Dianov et al. [64] observed and investigated the photoinduced SHG in a centrosymmetric ruby crystal. This thoroughly investigated crystal is an ideal medium for model investigations. Dianov et al. established a considerable difference between the photoinduced SHG and the effect associated with a photoelectric instability in the ruby crystal (see Section 3.3).

Organic materials are also promising media for photoinduced SHG. Charra et al. [65] discovered a transient nonlinearity in solutions of noncentrosymmetric molecules. Trapping of dipole-type chromophores in a polymer matrix enabled Charra et al. [66] to achieve a fairly stable photoinduced quadratic nonlinearity.

3. Experimental identification of the mechanism of the photoinduced second harmonic generation

It follows from this brief historical review of the topic that a fairly large number of experiments has been carried out and many different models have been proposed to account for the photoinduced SHG in glasses. The majority of these models have a clear physical meaning and the processes described by them may obviously be realised under certain conditions in systems of one kind or another. The general ideas on the physical properties of a medium and numerical estimates can serve to indicate which mechanisms of the effect are more probable. However, in our opinion, the nature of the quadratic nonlinearity in each specific case can be determined only on the basis of experiments in which the contributions of the various mechanisms can be separated. In this section we shall consider the experimental results which we think can throw light on the physical mechanisms leading to the photoinduced SHG.

3.1 Charge and orientational models

The models proposed to account for the photoinduced SHG can be divided into two groups: orientational and charge. An important feature of the orientational models is the assumption that an asymmetry of the electric-dipole type, associated with the quadratic susceptibility, exists in a medium at a microscopic level. The dipole moment D of a macroscopic region prepared for SHG consists of the vector sum of the aligned (or induced) contributions of separate microdipoles d_i which can be asymmetric molecules, structure defects, etc.:

$$D = \sum_i d_i. \quad (3)$$

In the simplest case the role of an external force is to orient along a given direction the randomly aligned dipole moments present in a medium [19]; hence the name for this group of models (Fig. 1a). In the charge models the quadratic susceptibility is induced by an electrostatic field [27, 17],

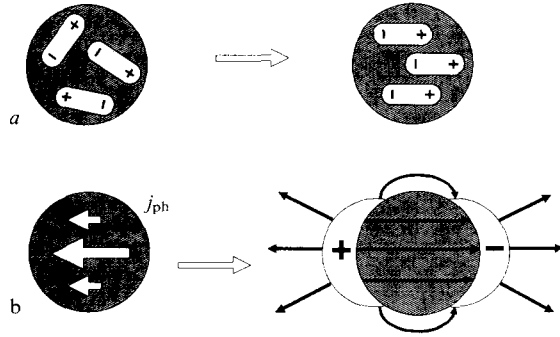


Figure 1. Photoinduced processes in the course of formation of a quadratic nonlinearity (the write fundamental-frequency and second-harmonic spots are shaded): (a) appearance, in the orientational models, of an asymmetry because of orientation (or formation) of microscopic dipoles within the write region; (b) formation of space-charge regions at the boundaries of an illuminated zone in models with macroscopic charge separation by the photocurrent j_{ph} .

which is associated with macroscopic charge separation (Fig. 1b). The term 'macroscopic separation' is understood to be the separation of charges to distances comparable with the dimensions of the illuminated region (of the order of several microns), in contrast to 'microscopic processes' in the orientational models, which are concentrated over distances comparable with the bond lengths (of the order of tenths of a nanometre). In the models with macroscopic separation the space charge is formed in macroscopic regions and the electrostatic field \mathcal{E} of these regions governs the quadratic nonlinearity:

$$\chi^{(2)} = 3\chi^{(3)}\mathcal{E}. \quad (4)$$

In contrast to the orientational models, in which the orienting influence of light aligns the dipoles and gives rise to the quadratic susceptibility only in the illuminated region, in the charge models the projecting lines of the electrostatic field of the space charge regions may give rise to an effective quadratic susceptibility quite far outside the illuminated zone (Fig. 1b).

Neither the experiments involving the application of an external field [28, 29] nor tensor measurements [37] have given an unambiguous answer to the question which of the mechanisms is responsible for the photoinduced SHG. To the best of our knowledge, the idea of distinguishing these two mechanisms and the corresponding experimental method were first proposed by us [46]. The difference between the orientational models and those based on charge separation lies in the important role played by the boundary of the illuminated region in macroscopic charge separation. If one of the space charges at the boundary or its sign is altered in some way, this also changes the electrostatic field and the quadratic susceptibility in the region between the charges. This effect on the charge, which appears after the preparation of a region in a bulk glass sample by focused pump and seeding second-harmonic beams, can be achieved if a prepared sample is displaced along the charge separation direction by a distance less than the distance between the charges.

In the case of the pump and seeding second-harmonic radiations polarised linearly in one plane the photogalvanic current is directed along the polarisation of the radiation

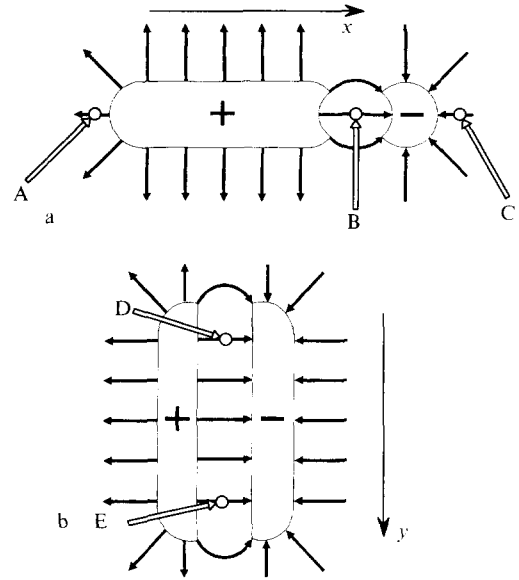


Figure 2. Schematic diagram showing charge separation and the electrostatic field lines, obtained for different directions of displacement (during the write process): along the charge separation direction (x axis, a) and perpendicular to this direction (y axis, b). The points labelled A, B, and C correspond to the maxima of the field along the x axis and the points labelled D and E correspond to the edges of an extended region along the y axis.

(specifically along the x axis). Repetition of the procedure of the preparation of a sample, carried out after its displacement in the same direction, should produce an extended region with a charge of the same sign separated from a small region of a charge with the opposite sign (Fig. 2a).

The electrostatic field \mathcal{E}_x , directed along the polarisation of light, and the corresponding components of the quadratic susceptibility tensor $\chi_{xxx}^{(2)} = 3\chi_{xyy}^{(2)}$ have three maxima: near the initial point at the edge of an extended space charge region with the same sign (point A); at a point B where the formation process is complete (between the space charge regions); and outside a small region with a charge of the opposite sign (point C). Near the extended space charge region the field component \mathcal{E}_y has a nonzero value; it is perpendicular to the direction of charge separation along the y axis and it leads to the corresponding components of the quadratic susceptibility tensor $\chi_{yyx}^{(2)} = 3\chi_{yxx}^{(2)}$.

A similar procedure of consecutive preparation of a sample with displacement perpendicular to the polarisation of the radiations (direction y) should ensure that the electrostatic field \mathcal{E}_x and the corresponding components of the quadratic susceptibility tensor $\chi_{xxx}^{(2)} = 3\chi_{xyy}^{(2)}$ remain constant throughout the prepared region D–E (Fig. 2b). However, if the dipoles are oriented or the charges are separated microscopically, it is possible to prepare a sufficiently extended region of $\chi^{(2)}$ by displacing a sample in an arbitrary direction. Therefore, an experiment involving the preparation of a sample in accordance with the method described above can give an unambiguous answer on the mechanism responsible for the quadratic nonlinearity.

Our investigation [46] was carried out on a sample of ZhS4 lead silicate glass. After the preparation of this sample by the proposed method, when a region of the glass formed by the procedure involving displacement along the direction of the polarisation of light was 'read' by the

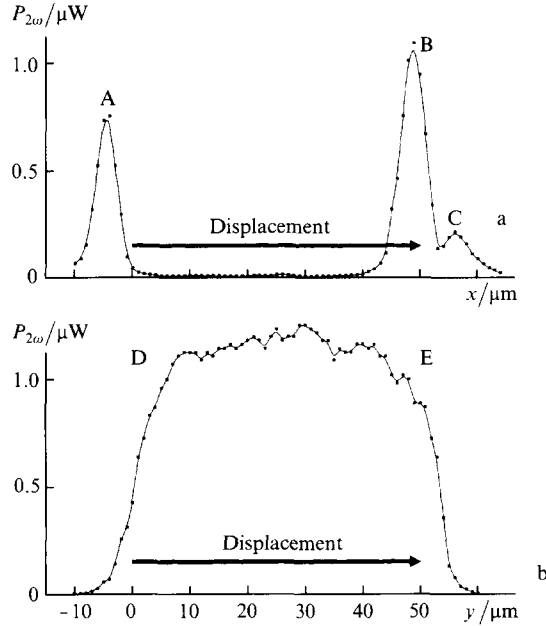


Figure 3. Dependences of the power of the photoinduced second harmonic, obtained for the displacement of regions in ZhS4 lead silicate glass, prepared by $\sim 50 \mu\text{m}$ displacement along the charge separation direction (a) and perpendicular to this direction (b). The positions of the points labelled A, B, C, D, and E are shown in Fig. 2.

pump beam, the results did indeed reveal three maxima of the second-harmonic intensity (Fig. 3a). A zero shift corresponded to the initial point in the preparation process. In the region between the two main maxima the shape of the spot had a characteristic split form, corresponding to the electrostatic field lines diverging from a space charge region located in the middle of the read spot. The intensity of the spot representing the photoinduced second harmonic in this region increased by a factor of ~ 10 when the polarisation of the read pump was rotated by 90° , i.e. the relationship $\chi_{yyy}^{(2)} = 3\chi_{yxx}^{(2)}$ was satisfied. The polarisation of the second-harmonic signal generated in this region was orthogonal to the polarisation of light used in the preparation of the sample. When the pump beam was used to read a region of this glass prepared by the procedure involving displacement in a direction perpendicular to the polarisation of light, the intensity of the second-harmonic signal was practically constant throughout the prepared region (Fig. 3b). Therefore, the results of this experiment on ZhS4 glass confirmed the occurrence of the macroscopic charge separation [46].

As pointed out already, Dominic and Feinberg [48] used a read beam to scan a region of a fibre preform prepared for SHG. The distribution of the electric field, deduced from the distribution of the intensity of the photoinduced second harmonic, provided further confirmation of the macroscopic charge separation reported in Ref. [46]. However, in experiments on glasses containing semiconductor nanocrystallites, extended regions with the quadratic nonlinearity were observed when a sample was displaced along and across the direction of the polarisation of light: the intensity of the second-harmonic signal was practically constant in both cases [46]. In our opinion, glasses doped with semiconductor nanocrystallites can be used as a model of an 'orientational' medium. Charge separation in such glasses

is possible within nanocrystallites of dimensions much less than the dimensions of the light beam. Such charge separation can be regarded as a form of 'orientation' of nanocrystallites.

3.2 Diffusion, optical rectification, and the photogalvanic effect

The mechanism responsible for charge separation is still an unsolved problem. The proposed mechanisms are the charge separation by diffusion, drift in an optical rectification field, and charge separation by the photogalvanic effect.

In models of the diffusion type the motion of charges is the consequence of nonuniformity of illumination of a sample, which leads to an inhomogeneity of the density of the photogenerated carriers [67, 68]. The density of the diffusion current tending to compensate this nonuniformity is

$$j = -\mathcal{D}\nabla\rho, \quad (5)$$

where \mathcal{D} is the carrier diffusion coefficient and ρ is the charge density. Typical fields created by the diffusion currents can reach $\sim 10^3 \text{ V cm}^{-1}$ [70, 59]. Obviously, after the completion of charge redistribution, the field configuration should be governed by the gradient of the intensity of the illuminating beam. In the diffusion models it is necessary to postulate the existence of higher spatial modes in order to specify the direction of charge separation [68]. Moreover, complications arise in the description of the required grating periodicity [59]. These properties are not in agreement with the published experimental data on the photoinduced SHG in single-mode fibre waveguides or with the data on the formation of a nonlinearity in bulk glass samples [46].

The optical rectification effect represents mixing of the pump and second-harmonic waves because of a cubic nonlinearity, giving rise to a polarisation at zero frequency. This mechanism was proposed by Stolen and Tom [19] to account for the photoinduced SHG. Physically, it is analogous to a familiar phenomenon, which is the optical rectification in a medium with a quadratic nonlinearity, but the participation of the waves with the frequencies ω and 2ω may create a static polarisation when the waves are mixed because of the cubic nonlinearity:

$$P_{dc} = \frac{3}{8}\epsilon_0\chi^{(3)}(0 = \omega + \omega - 2\omega)|E_\omega E_\omega E_{2\omega}^*| \cos(\Delta kz). \quad (6)$$

In its turn, this polarisation creates an electrostatic field which oscillates with a period necessary for quasi-phase-matched SHG:

$$\mathcal{E}_{dc} = \frac{P_{dc}}{\chi^{(1)}\epsilon_0} = \frac{3\chi^{(3)}}{8\chi^{(1)}}|E_\omega E_\omega E_{2\omega}^*| \cos(\Delta kz). \quad (7)$$

According to the models postulating the optical rectification as the cause of symmetry breaking, the field intensity should be sufficiently high to control the following elementary processes: orientation of the dipoles [19]; the Stark splitting of the absorption bands of centres oriented in different ways [22]; drift of charges [27, 69], etc. Numerical estimates indicate that the field intensity in silica glasses expected for the optical rectification mechanism is considerably less than that needed for a strong interaction with the medium: it is approximately 1 V cm^{-1} for typical intensities [28]. It has also been shown that the appearance of the quadratic nonlinearity requires much stronger fields

($\sim 10^4 \text{ V m}^{-1}$), and, therefore, the photogalvanic effect is the only real mechanism of the photoinduced appearance of the quadratic nonlinearity in such glasses.

The optical rectification effect can nevertheless be used to account for the photoinduced quadratic nonlinearity in a glass with semiconductor nanocrystallites [56] of dimensions typically from a few to a few tens of nanometres. The non-resonant cubic nonlinearity of the semiconductor is approximately two orders of magnitude greater than that of fused silica and at a resonance this difference is a factor of $\sim 10^5$. The optical rectification field may then separate charges by carrier drift and such separation may be retained in a glass when charges are captured by traps. According to Ref. [46], charge separation as a result of the coherent photogalvanic effect inside nanocrystals can account for the photoinduced SHG.

It therefore follows that the charge mechanism of the photoinduced SHG postulates two ways of charge separation: by the optical rectification field and by the photogalvanic effect. These ways are most difficult to distinguish in the case of glasses containing semiconductor nanocrystals, which should be associated with much higher optical rectification fields.

However, we think that the contribution of these two ways can be distinguished. There is a considerable difference between the photogalvanic and optical rectification effects only during the action of a write pulse [61, 62]. If the optical rectification effect predominates, the electrostatic field is maximal at the initial moment and then, as a quadratic nonlinearity grating is formed, the *drift current* of charges compensates for (reduces) the initial field.

Only in the case of the photogalvanic effect is the electrostatic field absent at the initial moment of grating formation and then it *rises continuously* as the grating evolves. Therefore, the field-induced quadratic susceptibility at the moment of action of a write pulse should fall only in the case of the optical rectification effect and should rise continuously if the photogalvanic mechanism is valid. If we bear in mind that the charges being separated are captured not only by the traps near the glass–semiconductor interface, but also penetrate partly into the glass, it is logical to expect the appearance of two different components, which are charac-

teristic of the rise and relaxation of the photoinduced second-harmonic signal: a fast component, representing the processes inside nanocrystallites, and a slow process associated with charges in the glass matrix.

Fig. 4 shows schematically the apparatus used in our study of the dynamics of the photoinduced quadratic nonlinearity at the moment of action of a write pulse [62]. Similar apparatus was probably used by Charra et al. [65] in an investigation of the nonlinearity induced in solutions of noncentrosymmetric dyes. In our experiments [62] we used a Q-switched and mode-locked YAG:Nd laser. Pulses of 600 ps duration were formed into packets of 30 pulses each and the pulse repetition frequency was 6.3 kHz. Seeding second-harmonic radiation was generated in a KTP crystal. The write and read radiations had the same polarisation, set by two Glan prisms. The read arm included a delay line which made it possible to ensure that the write and read pulses coincided in a sample.

Spatial filtering of the photoinduced second-harmonic signal, generated by a grating formed in a sample, made it possible to distinguish reliably the useful signal from the background associated with backward reflections of the seeding write radiation. The signal/background ratio was $\sim 10/1$. Special attention was paid to the spatial stability of the emission of the photoinduced second harmonic during these experiments.

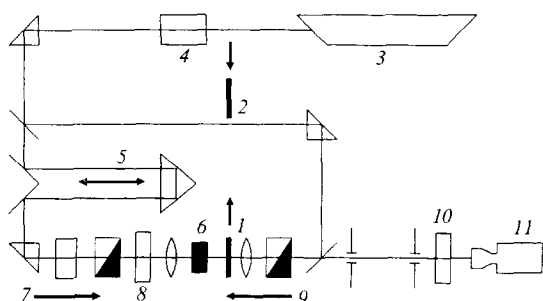


Figure 4. Schematic diagram of the apparatus used in an investigation of the dynamics of the quadratic nonlinearity during the action of a write pulse: (1, 2) shutters; (3) Q-switched mode-locked YAG:Nd laser; (4) KTP crystal; (5) delay line; (6) ZhS18 glass; (7) infrared read radiation; (8) infrared filter; (9) infrared write and second-harmonic radiations; (10) second-harmonic filter; (11) television camera. Opening of the first shutter (1) corresponds to the beginning of the write process and closing of the second shutter (2) corresponds to the completion of the process and erasure of the induced grating by the read radiation.

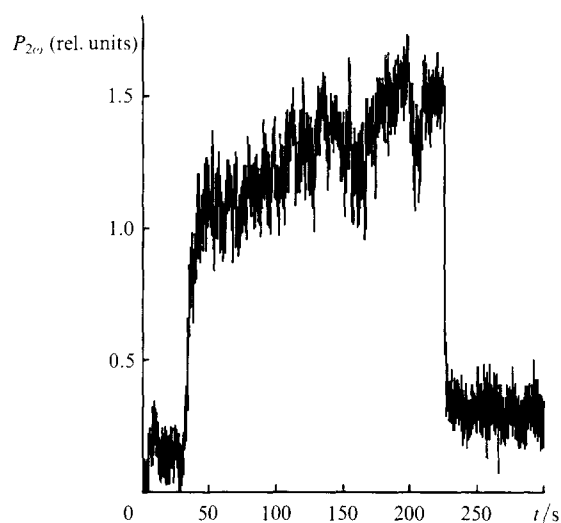


Figure 5. Time dependence of the photoinduced second-harmonic signal. The moment $t \approx 30 \text{ s}$ corresponds to the beginning and the moment $t \approx 230 \text{ s}$ corresponds to the end of the write process by the photoinduced second harmonic.

The experiments consisted of two stages: the write stage, beginning with the opening of a shutter (1) in front of an objective, and the stage of erasure of the induced nonlinearity by the read radiation, which began when the read radiation outside the signal arm was interrupted by a second shutter (2 in Fig. 4). The operating time of the shutters was $\sim 0.2 \text{ s}$ and the time resolution of the recording system, governed by a television camera, was $0.3\text{--}0.5 \text{ s}$. The experimental dependence of the photoinduced second-harmonic signal obtained for coinciding pulses is given in Fig. 5. Opening of the first shutter (1) at $t \approx 30 \text{ s}$ resulted in rapid growth of the second-harmonic signal and this was followed by a slower rise. Interruption by the second

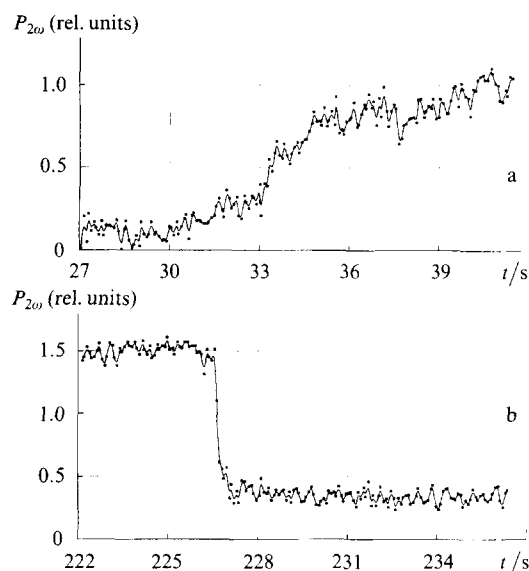


Figure 6. Time dependences of the fast component of the rise (a) and relaxation (b) of the photoinduced second-harmonic signal.

shutter (2) at $t \approx 220$ s resulted in very fast relaxation of the second harmonic, followed by a slower decay (the latter was characterised by a fairly large time constant, so that it was practically undetectable in Fig. 5). The residual second-harmonic signal was of the same order of magnitude as the increase in the signal because of the slow component. The fast component was observed only when the pulses coincided.

The photoinduced SHG efficiency reached $\sim 5 \times 10^{-9}$, which corresponded to a quadratic nonlinearity of $\sim 1.5 \times 10^{-16}$ m V $^{-1}$. The results of these experiments, involving reading of the nonlinearity at the moment of action of the write pulse, supported the photogalvanic model of the photoinduced SHG process: formation of a $\chi^{(2)}$ grating was accompanied by a continuous increase of the second-harmonic signal. Slow and fast components of this signal were observed (Fig. 5). The fast rise (Fig. 6a) and relaxation (Fig. 6b) components were attributed to transient $\chi^{(2)}$ gratings formed by the coherent photogalvanic effect in semiconductor nanocrystals embedded in glass. To the best of our knowledge, such dynamic quadratic-nonlinearity gratings were observed for the first time. Estimates indicated that under our experimental conditions the intensity of the optical rectification field was insufficient to create the observed nonlinearity.

The results obtained did not imply complete rejection of the optical rectification mechanism, which could occur at a resonance or in other systems, as well as at intensities higher than in our experiments.

3.3 Photogalvanic effect due to a photoelectric instability. The coherent photogalvanic effect

The mechanism of the photogalvanic effect resulting in charge separation has been the subject of lively discussions. The photogalvanic effect associated with a photoelectric instability, and the coherent photogalvanic effect, appearing because of a photoionisation asymmetry, have been proposed.

The idea of a mechanism based on a photoelectric instability and accounting for the appearance of a quadratic

nonlinearity by postulating a phase transition [71–73] is based on the assumption that a strong optical wave switches a system to a state far from equilibrium and that relaxation to an equilibrium state then disturbs the symmetry. This relaxation is accompanied by the appearance of a current which enhances the electrostatic field. The initial electrostatic interaction may be created by, for example, the optical rectification effect and it may lead to the formation of a $\chi^{(2)}$ grating with the required periodicity. It has frequently been pointed out that this mechanism is analogous to that proposed for the description of the photoinduced fields in a ruby crystal [70, 74]. Until recently this type of the photogalvanic effect has been observed only in ruby.

The appearance of a current along a given direction requires the presence of ions at polar positions along this direction (which is the crystallographic X_3 axis in ruby). A photoelectric instability in ruby has the properties typical of phase transitions: the effect is observed only at low temperatures ($T < 150$ K), when a certain threshold concentration ($\sim 3 \times 10^{19}$ cm $^{-3}$) of chromium ions is exceeded, and only in a certain range of intensities. An important feature of the photogalvanic current is that it can be directed *only along the orientation axis of dipole centres* (X_3 axis in ruby). Similarly, the photogalvanic current in the photoinduced SHG models, based on a photoelectric instability, should also appear only along the direction of orientation of the dipoles.

In the case of the coherent photogalvanic effect the presence of ions at polar positions is not an essential condition for the appearance of the current. Therefore, charge separation may occur, depending on the polarisation of the write radiation, along different directions. Since centres of the dipole type are oriented randomly in glass, it is difficult to propose a clear experiment which would reveal the difference between the two effects. Obviously, the most appropriate medium for identifying the nature of the photogalvanic effect resulting in the photoinduced SHG is a system with a given orientation of the dipole centres, such as a ruby crystal.

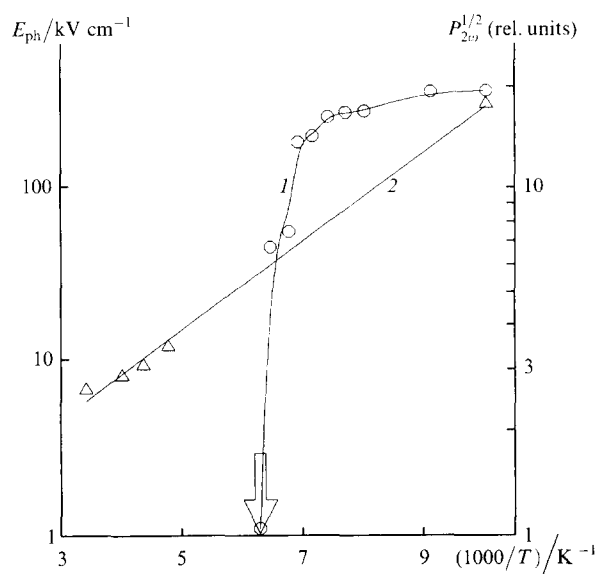


Figure 7. Temperature dependences of: (1) the electrostatic field due to the photogalvanic effect associated with a photoelectric instability [70]; (2) the quantity $P_{2\omega}^{1/2}$ proportional to the electrostatic field in the photoinduced SHG in ruby [64].

Studies of the photoinduced SHG in ruby have shown that the direction of charge motion can be perpendicular to the axis X_3 of orientation of the dipole centres and can be governed by the polarisation of the write radiation [64]. The concentration and temperature dependences of the photoinduced SHG in ruby (Fig. 7) also differ considerably from the dependences typical of a phase transition. Therefore, the results obtained support unambiguously the coherent photogalvanic effect.

3.4 Order of the coherent photogalvanic effect

One of the important questions relating to the mechanism of the coherent photogalvanic effect, which leads to the photoinduced SHG, is how many coherent photons participate in the asymmetric photoionisation process. The understanding of this mechanism is very important for practical applications of the photoinduced SHG. We shall now consider in greater detail a phenomenological description of the photogalvanic effect.

The coherent photogalvanic (photovoltaic) effect represents the appearance of a current in a medium (which may be centrosymmetric or noncentrosymmetric) as a result of uniform illumination. The photoinduced SHG is attributed to the appearance of a current when a sample is illuminated with the fundamental-frequency and second-harmonic radiations [33, 17]. The coherent photogalvanic effect is similar to the bulk photogalvanic effect which appears in noncentrosymmetric media [70]. Since the density of the coherent photogalvanic current depends on the phase relationships between the optical waves which induce it, it follows that a steady-state current appears if the waves are mutually coherent and this is why it is called the coherent effect. The phenomenological approach yields the following expression for the density of the photogalvanic current induced by waves of frequencies ω and 2ω [62]:

$$\begin{aligned} j_{ph} = & \beta_b(E_\omega E_\omega^* + E_{2\omega} E_{2\omega}^*) + \beta E_\omega E_\omega E_{2\omega}^* \exp(i\Delta kz) + \\ & + \beta_1 E_\omega E_\omega E_\omega E_{2\omega}^* \exp(i\Delta kz) + \\ & + \beta_2 E_\omega E_\omega E_{2\omega} E_{2\omega}^* \exp(i\Delta kz) + \\ & + \beta_3 E_\omega E_\omega E_\omega E_\omega E_{2\omega}^* \exp(i\Delta kz) + \dots + \text{c. c.} \end{aligned} \quad (8)$$

Here, the first component represents the bulk photogalvanic effect [70] (which is absent from glasses because they are centrosymmetric). The second component is the coherent photogalvanic effect of the lowest order, which involves the participation of three coherent photons and appears because of interference between two-photon ionisation by the fundamental-frequency radiation and one-photon ionisation by the second harmonic [17, 33, 34].

The third and other components represent the coherent photogalvanic effect of higher orders, which involves the participation of more than three coherent photons. For example, the fifth component (corresponding to the seventh-order effect) is due to interference between four-photon ionisation by the fundamental-frequency radiation and three-photon ionisation involving two fundamental-frequency photons and one second-harmonic photon [36].

In the coherent processes each additional coherent photon reduces the probability of the process by the factor $\sim E/E_{at}$. For typical intensities used in the experiments this factor amounts to $\sim 10^{-2}$. The photogalvanic coefficients $\beta_b, \beta, \beta_1, \beta_2, \beta_3$ depend on the concentrations of the

relevant photogalvanic centres (defects or states from which asymmetric photoionisation of the relevant order originates).

A constant electrostatic field \mathcal{E}_{dc} forms in a medium as a result of compensation of the photogalvanic current by the drift current: $\mathcal{E}_{dc} = -j_{ph}/\sigma$, where σ is the photoconductivity. This field induces the quadratic nonlinearity and the rise of the latter is described by the equation

$$\frac{\partial \chi^{(2)}}{\partial t} = A - \frac{\chi^{(2)}}{\tau}, \quad (9)$$

where $\tau = \epsilon\epsilon_0/\sigma$; ϵ is the relative permittivity of the medium; ϵ_0 is the permittivity of vacuum; $A \propto \chi^{(3)}j_{ph}/\epsilon\epsilon_0$. During the initial stage, when relaxation can be ignored (because $\chi^{(2)}$ is small) the rise of the quadratic susceptibility is linear and, therefore, the time dependence of the second-harmonic signal can be approximated by the quadratic expression:

$$I_{ph}(2\omega) = \Gamma t^2 + \text{const}. \quad (10)$$

The rate parameter $\Gamma \propto A^2$ depends on the order of the process, and on the intensities of the write and read waves:

$$\begin{aligned} \Gamma \propto A^2 (I_\omega^r)^2 \propto & \beta^2 (I_\omega^w)^2 I_{2\omega}^w (I_\omega^r)^2 + \beta_1^2 (I_\omega^w)^4 I_{2\omega}^w (I_\omega^r)^2 + \\ & \beta_2^2 (I_\omega^w)^2 (I_{2\omega}^w)^3 (I_\omega^r)^2 + \beta_3^2 (I_\omega^w)^6 I_{2\omega}^w (I_\omega^r)^2 + \dots, \end{aligned} \quad (11)$$

where I_ω^r is the intensity of the read radiation; I_ω^w and $I_{2\omega}^w$ are the intensities of the write pump and second-harmonic radiations, respectively. An investigation of the dependence of Γ on the intensities makes it possible to determine the order of the nonlinear process which generates a grating of $\chi^{(2)}$.

The photoinduced SHG, which appears because of the high energy of photoionisation of germanium defects in glasses, is explained in Ref. [36] on the basis of the higher-order components of the coherent photocurrent. The power exponents of the experimental dependences of the rate of growth on the intensities of the write pump and second-harmonic waves are described better by the models which consider the higher orders of the coherent photocurrent [54, 55]. However, a different explanation is also possible without invoking the higher orders of the coherent photocurrent involving more than three photons.

In fact, the photogalvanic constant β for the lowest-order coherent photocurrent depends on the concentration of photogalvanic centres [31]. Such centres may be created by coherent or incoherent radiation. Intermediate states can also act as such centres. In this case the photogalvanic constant β depends on the intensities of the write waves. The existence of intermediate metastable states is supported by experiments involving pulsed [49] and continuous [75, 76] ultraviolet irradiation of germanium-doped fibre waveguides. Creation of photogalvanic centres (filling of intermediate states from which the asymmetric photoionisation originates) by the write fundamental-frequency and second-harmonic waves increases, because of their incoherent contribution, the power exponents in the expressions describing the dependences of the rate of growth on the wave intensities. If intermediate states are filled in some way, the order of the process may be reduced and it may become equal to the order of the coherent process.

We proposed and carried out experiments on counter-propagating write and read pulses used to fill intermediate states by the read pump radiation with the aim of finding the order of the coherent process [77, 78]. We investigated ZhS4 lead silicate glass doped with cerium. The apparatus (Fig. 8) was similar to that employed in the reading of the

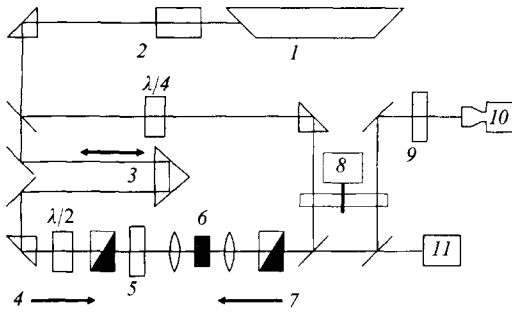


Figure 8. Schematic diagram of the apparatus used in an investigation of filling of intermediate states by counterpropagating read radiation beams involving the use of the $\lambda/4$ ($\lambda = 532$ nm) and $\lambda/2$ ($\lambda = 1064$ nm) plates for varying the power of, respectively, the infrared write and read radiations: (1) Q-switched mode-locked YAG:Nd laser; (2) KTP crystal; (3) delay line; (4) infrared read radiation; (5) infrared filter; (6) ZnS4 glass; (7) infrared write radiation and second harmonic; (8) chopper; (9) second-harmonic filter; (10) television camera; (11) device for monitoring the pulses.

nonlinearity at the moment of action of an optical pulse. Small signals were recorded with the aid of a mechanical chopper. The chopper disk interrupted periodically the write arm and simultaneously opened an aperture which allowed the photoinduced second-harmonic signal to reach the recording system. This made it possible to avoid the influence of back reflection of the write second-harmonic radiation. Similar apparatus was used by Kamal et al. [54] in a study of the rate of growth in fibre waveguides, but in their case the write and read pulses did not overlap.

We investigated the dependence of the degree of saturation of the second-harmonic signal on the delay of the read pulse. When an intermediate state with a short (compared with the pulse duration) lifetime is filled, this dependence should have the Gaussian profile with the maximum for the coincident pulses. Filling of a state with a sufficiently long lifetime should alter the form of the dependence because of the delay and should give rise to a relaxation tail. If intensity of the radiation filling the state is sufficiently high, the dependence should have a characteristic flat top on attainment of population saturation.

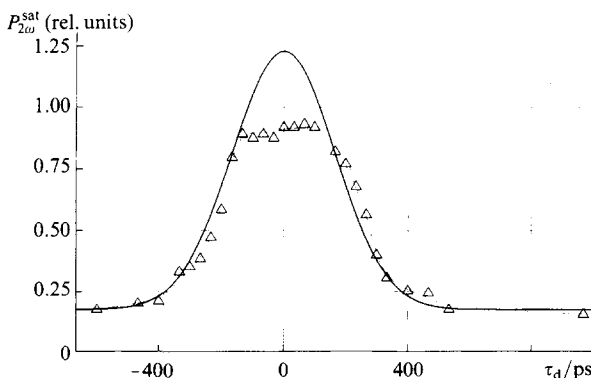


Figure 9. Dependence of the power of the saturated photoinduced second harmonic on the delay of the read pulse, obtained for an average read power of 900 mW, delivered in the form of pulses of ~ 600 ps duration when the average infrared write power was 70 mW and the power of the write second harmonic was ~ 400 μ W. The approximation of the experimental curve by a Gaussian profile reveals the distortion of the experimental curve.

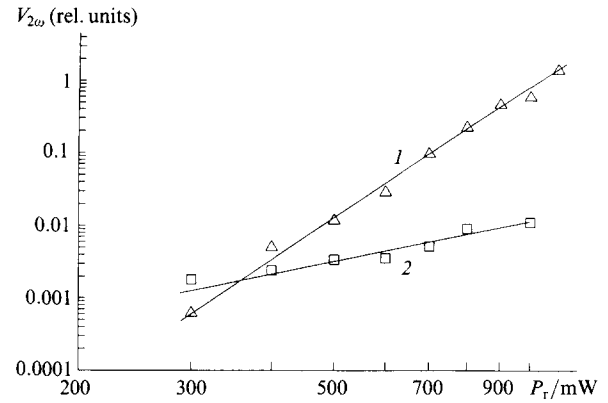


Figure 10. Dependence of the initial rate of growth of the photoinduced second harmonic $V_{2\omega}$, in the case of coincident (1) and noncoincident (2) pulses, on the read radiation power when the write radiation power was 70 mW. The experimental dependences are approximated by power-law dependences with the power exponents 6 and 1.9 for the coincident ($\tau_d = 0$) and noncoincident ($\tau_d = 800$ ps) pulses, respectively.

The experimental dependence of the power of the saturated second-harmonic signal on the delay of the read pulse is shown in Fig. 9. When the write and read pulses coincided, there was a considerable increase in power of the saturated second harmonic and a reduction in the write time. According to the photogalvanic model, this was evidence of an increase in the photogalvanic current. A change in the profile of the dependence, corresponding (in our opinion) to saturation of an intermediate state with a short lifetime, was demonstrated by the Gaussian approximation of the resultant dependence. A higher precision would be needed in a more detailed study of these intermediate states.

The differences between the write processes in the case of coincident and noncoincident pulses were identified by investigating the dependences of the initial growth rate on the powers of the write and read infrared radiations. The dependences on the power of the read radiation are plotted in Fig. 10. For noncoincident pulses the dependence was nearly quadratic (with the power exponent 1.9 ± 0.4). Hence, the pump radiation did not affect the write process. When the pulses coincided, the power exponent increased to almost 6 (5.8 ± 0.6). This increase by 4 in the power exponent of the dependence corresponded to a two-photon contribution of the read radiation to filling of the investigated intermediate state:

$$\Gamma(I_r) \propto \beta^2 I_r^2(\omega) \propto [I_r^2(\omega)]^2 I_r^2(\omega). \quad (12)$$

It also follows from Fig. 10 that the rate of growth increased approximately 100-fold when the pulses coincided.

Similar dependences of the initial growth rate of the photoinduced second harmonic on the write infrared power are plotted in Fig. 11. When the pulses coincided, the intermediate state was filled mainly by the read pump radiation and the power exponent of the dependence decreased, assuming the value corresponding to the lowest-order coherent photogalvanic effect: 1.8 ± 0.5 . In this case a quadratic nonlinearity grating could be prepared at extremely low write infrared radiation powers (peak power less than 60 W). In the case of noncoincident pulses the power exponent of the dependence tended to 6 (5.2 ± 0.8), which corresponded to filling

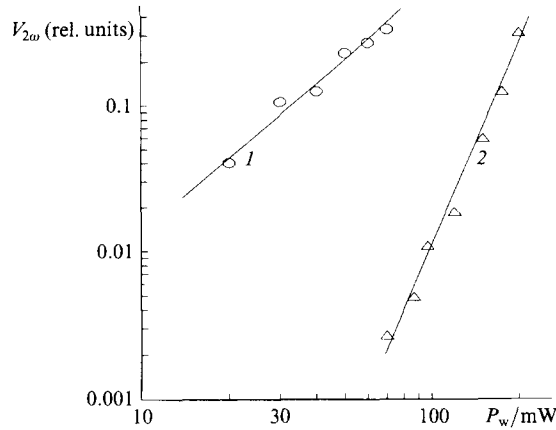


Figure 11. Dependences of the initial rate of growth of the photoinduced second harmonic $V_{2\omega}$, in the case of coincident (1) and noncoincident (2) pulses, on the write pump power when the infrared read power was 1 W. The experimental dependences are approximated by power-law dependences with the power exponents 5.4 and 1.7 for the coincident ($\tau_d = 0$) and noncoincident ($\tau_d = 800$ ps) pulses, respectively.

of the intermediate states by the write infrared photons:

$$\Gamma(I_w) \propto \beta^2 I_w^2(\omega) \propto [I_w^2(\omega)]^2 I_w^2(\omega). \quad (13)$$

In our opinion, these experiments [77] proved two-photon filling of an intermediate state by the fundamental-frequency radiation and confirmed the lowest-order coherent photogalvanic effect starting from this state (Fig. 12).

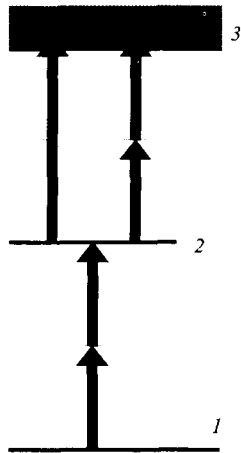


Figure 12. Energy band diagram illustrating the lowest-order coherent photogalvanic effect from a defect level (1) and involving two-photon filling of an intermediate state (2), followed by a transition to the conduction band (3).

4. Promising glasses for the photoinduced second-harmonic generation

The development of practical devices based on the photoinduced SHG will require new materials with a much stronger photoinduced quadratic nonlinearity and lower write radiation powers. One of the possible ways of increasing the photoinduced SHG efficiency is to find materials with a higher coherent photocurrent density. This can be done by increasing the concentration of photogalvanic centres. Experiments on filling of intermediate states by

counterpropagating beams show that an increase in the current density, for given write wave intensities, is achieved by reducing the order of the grating-formation process. Moreover, it should be possible to form $\chi^{(2)}$ gratings at much lower intensities.

In germanium-doped silica glass the photoinduced SHG is associated with oxygen-deficit centres. The concentration of these structure defects in glasses depends on the conditions during the synthesis and treatment of glass, so that it is quite difficult to control quantitatively this concentration. Moreover, the absorption band of such centres lies in the region of 240 nm. This means that the most probable (third-order) coherent process, resulting in asymmetric photoionisation, is possible only from an intermediate excited state and the filling of this state increases the order of the whole process.

An interesting alternative to oxygen-deficit centres is the variable-valence ions which in the chemically reduced form can be photoelectron donors and in the oxidised form can act as traps [79]. It has been reported that efficient photoinduced SHG is possible in aluminosilicate fibre waveguides doped with rare-earth elements [53, 79–82].

We think that the selection of a dopant and of a suitable glass matrix can produce a material which has a photosensitivity in the required spectral range. Zel'dovich et al. [44] detected efficient photoinduced SHG in lead silicate glass. Even more efficient photoinduced SHG has been observed and studied in lead germanate glasses doped with cerium ions [63]. The gratings in these glasses were formed by radiation from a Q-switched mode-locked YAG:Nd laser. Seeding second-harmonic radiation was generated in a KTP crystal. The photoinduced SHG was not observed in lead germanate glasses with different compositions belonging to the $\text{PbO}-\text{GeO}_2$ system without additional impurities. It is possible that an important condition for the appearance of strong photoinduced fields is, as in the case of the photorefractive effect [70], the occurrence of considerable fluctuations of the local potential which ensure that the transport properties of cold and hot carriers are different.

A comparison of glasses with the molar PbO concentrations of 10%, 20%, 30%, and 40%, containing 0.25% of cerium oxide by weight showed that, under identical conditions, the glasses with 20%, 30%, and 40% of PbO

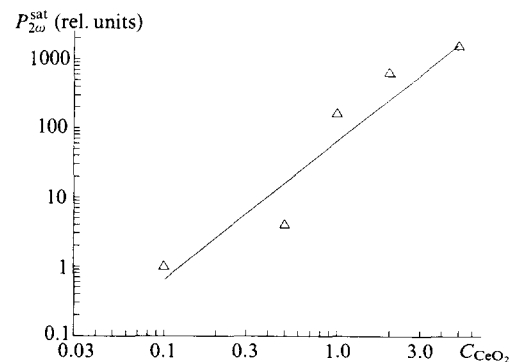


Figure 13. Dependence of the power of the saturated photoinduced second harmonic on the concentration of CeO_2 in a lead germanate glass of the $\text{PbO}:\text{GeO}_2 = 20:80$ composition. The quadratic approximation to the dependence demonstrates a linear increase in the photoinduced nonlinearity with increase in the Ce concentration.

had similar levels of saturation of the photoinduced second-harmonic signal, whereas the sample with 10% PbO was much less effective. An increase in the PbO concentration reduced the power at which optical breakdown took place and, therefore, further investigations were carried out by us on a system of the $\text{PbO}:\text{GeO}_2 = 20:80$ composition. We studied the photoinduced SHG in samples with different Ce concentrations. An increase in the saturation level of the second-harmonic signal with increase in the Ce concentration was described quite well by the quadratic dependence, which corresponded to a linear increase in the quadratic nonlinearity (Fig. 13). We concluded that the contribution of cerium was related to the formation of photogalvanic centres.

The sensitivity of the samples with high Ce concentrations was considerably higher than the sensitivity of glass fibre preforms and of lead glasses. The levels of the saturation of the second-harmonic signal observed when the write pump power was increased are compared in Fig. 14 for a glass fibre preform with 8% GeO_2 , ZhS4 lead silicate glass doped with cerium, and lead germanate glass with a high concentration of Ce.

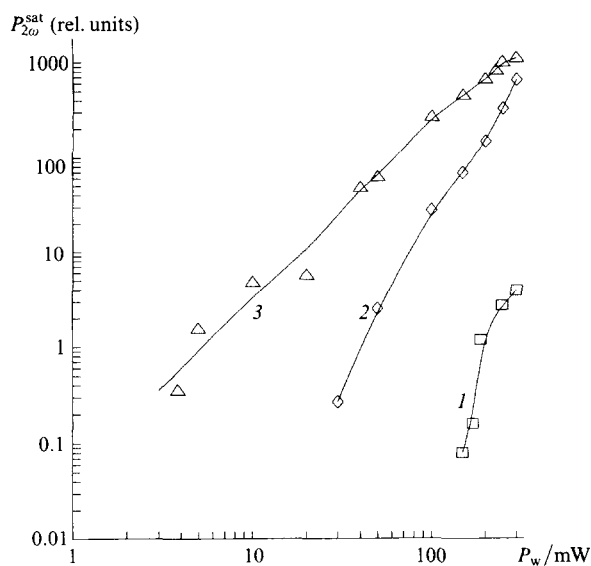


Figure 14. Dependences of the degree of saturation of the photoinduced second harmonic on the infrared write power obtained for: (1) fibre glass preform, containing 8% GeO_2 ; (2) ZhS4 lead silicate glass doped with Ce; (3) G2059 lead germanate glass with a high concentration of Ce. The infrared read power was 300 mW and the second-harmonic write power was 1 mW.

The dependence obtained for a lead germanate glass has the gentlest slope and, in our opinion, this corresponds to lower order of the grating-formation process. The quadratic nonlinearity can appear in this system at a power of the write radiation almost an order of magnitude less than in the case of lead silicate glasses and approximately two orders of magnitude less than for glass fibre preforms. The photoinduced second-harmonic signal was observed by us in G2059 experimental glass at a peak infrared write radiation power less than 30 W, which was comparable with the power (less than 60 W) found when the order of the write process by filling an intermediate state was reduced and the lowest-order coherent photogalvanic effect in ZhS4 lead silicate glass

was observed [77]. These results demonstrate that lead germanate glasses with high Ce concentrations are promising materials for practical devices.

5. Conclusions

The experimental data available at present demonstrate that the photoinduced SHG in glasses is due to charge separation as a result of the coherent photogalvanic effect. The microscopic nature of the coherent photocurrent, the photoionisation asymmetry, and the transport of charge in glasses are not yet fully understood. However, the explosive growth of this topic, which began in 1986, gives us grounds for expecting the understanding of these processes and the practical utilisation of the effect to be realised in the nearest future.

References

1. Franken P A, Hill A E, Peters C W, Weinreich G *Phys. Rev. Lett.* **7** 118 (1961)
2. Terhune R W, Maker P D, Savage C M *Phys. Rev. Lett.* **8** 404 (1962)
3. Terhune R W, Weinberger D A *J. Opt. Soc. Am.* **B** 4 661 (1987)
4. Fujii Y, Kawasaki B S, Hill K O, Johnson D C *Opt. Lett.* **5** 48 (1980)
5. Sasaki Y, Ohmori Y *Appl. Phys. Lett.* **39** 466 (1981)
6. Österberg U, Margulis W *Opt. Lett.* **11** 516 (1986)
7. MacDonald R L, Lawandy N M *Opt. Commun.* **103** 345 (1993)
8. Stolen R H, in *Nonlinear Waves in Solid State Physics* (Eds A D Boardman, M Bertolotti, T Twardowski; NATO ASI Series B: Physics, Vol. 227) (New York: Plenum Press, 1990) p. 297
9. Russell P St J, Hand D P, Poyntz-Wright L J *Proc. SPIE Int. Soc. Opt. Eng.* **1373** 126 (1990)
10. Sokolov V O, Sulimov V B *Izv. Akad. Nauk SSSR Ser. Fiz.* **54** 2313 (1990)
11. Glushchenko V Yu, Smirnov V B *Opt. Spektrosk.* **72** 990 (1992) [*Opt. Spectrosc. (USSR)* **72** 538 (1992)]
12. Österberg U, Margulis W *Opt. Lett.* **12** 57 (1987)
13. Farries M C, Russell P St J, Fermann M E, Payne D N *Electron. Lett.* **23** 322 (1987)
14. Tom H W K, Stolen R H, Aumiller G D, Pleibel W *Opt. Lett.* **13** 512 (1988)
15. Fermann M E, Farries M C, Russell P St J, Poyntz-Wright L J *Opt. Lett.* **13** 282 (1988)
16. Batdorf B, Krautschik C, Österberg U, Stegeman G, Leitch J W, Rotgé J R, Morse T F *Opt. Commun.* **73** 393 (1989)
17. Dianov E M, Kazanskii P G, Stepanov D Yu *Kvantovaya Elektron. (Moscow)* **16** 887 (1989) [*Sov. J. Quantum Electron.* **19** 575 (1989)]
18. Kamal A, Weinberger D A, Weber W *Opt. Lett.* **15** 613 (1990)
19. Stolen R H, Tom H W K *Opt. Lett.* **12** 585 (1987)
20. Dianov E M, Prokhorov A M, Sokolov V O, Sulimov V B *Pis'ma Zh. Eksp. Teor. Fiz.* **50** 13 (1989) [*JETP Lett.* **50** 13 (1989)]
21. Chmela P *Opt. Lett.* **13** 669 (1988)
22. Lesche B J *J. Opt. Soc. Am.* **B** 7 53 (1990)
23. Poyntz-Wright L J, Russell P St J *Technical Digest of Papers presented at Integrated Photonics Research Conference, Hilton Head, SC, 1990* (Technical Digest Series, Vol. 5) (Washington, DC: Optical Society of America, 1990) Paper MJ4, p. 47
24. Emel'yanov V I, Taeshnikov A B *Kvantovaya Elektron. (Moscow)* **18** 266 (1991) [*Sov. J. Quantum Electron.* **21** 236 (1991)]
25. Sokolov V O, Sulimov V B *Sov. Lightwave Commun.* **1** 419 (1991)
26. Dianov E M, Sokolov V O, Sulimov V B *Tr. Inst. Obshch. Fiz. Akad. Nauk* **39** 39 (1993)
27. Ouellette F, Hill K O, Johnson D C *Opt. Lett.* **13** 515 (1988)
28. Mizrahi V, Österberg U, Sipe J E, Stegeman G I *Opt. Lett.* **13** 279 (1988)
29. Mizrahi V, Österberg U, Krautschik C, Stegeman G I, Sipe J E, Morse T F *Appl. Phys. Lett.* **53** 557 (1988)

30. Dianov E M, Kazanskiĭ P G, Stepanov D Yu *Kvantovaya Elektron. (Moscow)* **17** 926 (1990) [*Sov. J. Quantum Electron.* **20** 849 (1990)]
31. Dianov E M, Kazansky P G, Stepanov D Yu *Sov. Lightwave Commun.* **1** 247 (1991)
32. Baskin É M, Éntin M V *Pis'ma Zh. Eksp. Teor. Fiz.* **48** 554 (1988) [*JETP Lett.* **48** 601 (1988)]
33. Éntin M V *Fiz. Tekh. Poluprovodn.* **23** 1066 (1989) [*Sov. Phys. Semicond.* **23** 664 (1989)]
34. Baranova N B, Zel'dovich B Ya, Chudinov A N, Shul'ginov A A *Zh. Eksp. Teor. Fiz.* **98** 1857 (1990) [*Sov. Phys. JETP* **71** 1043 (1990)]
35. Baranova N B, Beterov I M, Zel'dovich B Ya, Ryabtsev I I, Chudinov A N, Shul'ginov A A *Pis'ma Zh. Eksp. Teor. Fiz.* **55** 431 (1992) [*JETP Lett.* **55** 439 (1992)]
36. Anderson D Z, Mizrahi V, Sipe J E *Opt. Lett.* **16** 796 (1991)
37. Mizrahi V, Hibino Y, Stegeman G *Opt. Commun.* **78** 283 (1990)
38. Margulis W, Carvalho I C S, von der Weid J P *Opt. Lett.* **14** 700 (1989)
39. Koch K W, Moore G T *Proc. SPIE Int. Soc. Opt. Eng.* **1516** 67 (1991)
40. Bolshtyansky M A, Churikov V M, Kapitzky Yu E, Savchenko A Yu, Zel'dovich B Ya *Opt. Lett.* **18** 1217 (1993)
41. Dianov E M, Kazansky P G, Starodubov D S, Stepanov D Yu *Sov. Lightwave Commun.* **1** 395 (1991)
42. Krol D M, Broer M M, Nelson K T, Stolen R H, Tom H W K, Pleibel W *Opt. Lett.* **16** 211 (1991)
43. Lawandy N M, Selker M D *Opt. Commun.* **77** 339 (1990)
44. Zel'dovich B Ya, Kapitskiĭ Yu E, Churikov V M *Pis'ma Zh. Eksp. Teor. Fiz.* **53** 77 (1991) [*JETP Lett.* **53** 78 (1991)]
45. Dianov E M, Kazansky P G, Krauschik C, Stepanov D Yu *Sov. Lightwave Commun.* **1** 381 (1991)
46. Dianov E M, Kazansky P G, Starodubov D S, Stepanov D Yu *Sov. Lightwave Commun.* **2** 83 (1992)
47. Dianov E M, Kazansky P G, Starodubov D S, Stepanov D Yu *Sov. Lightwave Commun.* **2** 269 (1992)
48. Dominic V, Feinberg J *Opt. Lett.* **18** 784 (1993)
49. Carvalho I C S, Margulis W, Lesche B *Opt. Lett.* **16** 1487 (1991)
50. Ouellette F, Hill K O, Johnson D C *Appl. Phys. Lett.* **54** 1086 (1989)
51. Krol D M, Atkins R M, Lemaire P J *Proc. SPIE Int. Soc. Opt. Eng.* **1516** 38 (1991)
52. Saeta P N, Krol D M, DiGiovanni D J *Proc. SPIE Int. Soc. Opt. Eng.* **2044** 18 (1993)
53. Krol D M, DiGiovanni D J, Pleibel W, Stolen R H *Opt. Lett.* **18** 1220 (1993)
54. Kamal A, Terhune R W, Weinberger D A *Proc. SPIE Int. Soc. Opt. Eng.* **1516** 137 (1991)
55. Dominic V, Feinberg J *Opt. Lett.* **17** 1761 (1992)
56. Lawandy N M, MacDonald R L *J. Opt. Soc. Am. B* **8** 1307 (1991)
57. MacDonald R L, Lawandy N M *Electron. Lett.* **27** 2331 (1991)
58. MacDonald R L, Lawandy N M *Phys. Rev. B* **47** 1961 (1993)
59. Driscoll T J, MacDonald R L, Lawandy N M *Phys. Rev. A* **48** 3278 (1993)
60. Dianov E M, Kazansky P G, Starodubov D S, Stepanov D Yu *SPIE Int. Soc. Opt. Eng.* **2044** 11 (1993)
61. Dianov E M, Kazanskiĭ P G, Starodubov D S, Stepanov D Yu *Tezisy IV Mezhdun. Konf. 'Fizicheskie Problemy Opticheskikh Izmerenii, Svyazi i Obrabotki Informatsii', Sevastopol, 1993* (Abstracts of Papers presented at Fourth International Conference on Physical Problems in Optical Measurements, Communications, and Data Processing, Sevastopol, 1993) p. 12
62. Dianov E M, Kazanskiĭ P G, Starodubov D S *Kvantovaya Elektron. (Moscow)* **21** 685 (1994) [*Quantum Electron.* **24** 632 (1994)]
63. Dianov E M, Starodubov D S, Izyneev A A *Opt. Lett.* **19** 936 (1994)
64. Dianov E M, Kazansky P G, Prokhorov A M, Starodubov D S, Stepanov D Yu *Sov. Lightwave Commun.* **2** 157 (1992)
65. Charra F, Devaux F, Nunzi J M, Raimond P *Phys. Rev. Lett.* **68** 2440 (1992)
66. Charra F, Kajzar F, Nunzi J M, Raimond P, Idiart E *Opt. Lett.* **18** 941 (1993)
67. Lawandy N M *Opt. Commun.* **74** 180 (1989)
68. Anderson D Z *Proc. SPIE Int. Soc. Opt. Eng.* **1148** 186 (1989)
69. Bolshtyanskiĭ M A, Zel'dovich B Ya, Kapitskiĭ Yu E, Savchenko A Yu, Churikov V M *Kvantovaya Elektron. (Moscow)* **19** 1136 (1992) [*Sov. J. Quantum Electron.* **22** 1062 (1992)]
70. Sturman B I, Fridkin V M *Fotogal'vanicheskiĭ Éffekt v Sredakh bez Tsentra Simmetrii i Rodstvennye Yavleniya* (Photogalvanic Effect in Noncentrosymmetric Media and Related Phenomena) (Moscow: Nauka, 1992)
71. Dyakonov M I, Furman A S *Electron. Lett.* **27** 1429 (1991)
72. Emel'yanov V I *Trudy XIV Mezhdunar. Konf. po Kogerentnoi i Nelineinoi Optike, Leningrad, 1991* (Proceedings of Fourteenth International Conference on Coherent and Nonlinear Optics, Leningrad, 1991) Paper SWH4
73. Sokolov V O, Sulimov V B *Sov. Lightwave Commun.* **2** 301 (1992)
74. Liao P F, Glass A M, Humphrey L M *Phys. Rev. A* **22** 2276 (1980)
75. Driscoll T J, Lawandy N M *Opt. Lett.* **17** 571 (1992)
76. Dianov E M, Kazansky P G, Prokhorov A M, Starodubov D S, Stepanov D Yu *Sov. Lightwave Commun.* **2** 147 (1992)
77. Dianov E M, Kazansky P G, Starodubov D S *Sov. Lightwave Commun.* **3** 247 (1993)
78. Dianov E M, Kazansky P G, Starodubov D S *Technical Digest of Papers presented at Conference on Lasers and Electro-Optics, Anaheim, CA, 1994* (Technical Digest Series, Vol. 8) (Washington, DC: Optical Society of America, 1994) Paper CFC6, p. 400
79. Krol D M, Simpson J R *Opt. Lett.* **16** 1650 (1991)
80. Lawandy N M, Bernardin J P, Demouchy G, MacDonald R L *Electron. Lett.* **27** 1264 (1991)
81. Driscoll T J, Lawandy N M, Killian A, Reinhart L, Morse T F *Electron. Lett.* **27** 1729 (1991)
82. Dianov E M, Kornienko L S, Rybaltovsky A O, Chernov P V, Yatsenko Yu E *Opt. Lett.* **19** 439 (1994)